CD95 triggers Orai1-mediated localized Ca^{2+} entry, regulates recruitment of protein kinase C (PKC) β2, and prevents death-inducing signaling complex formation

Nadine Khadra[a,1], Laurence Bresson-Bepoldin[b,1], Aubin Penna[c], Benjamin Chaigne-Delalande[d], Bruno Ségui[e], Thierry Levade[e], Anne-Marie Vacher[b], Josy Reiffers[b], Thomas Ducret[f], Jean-François Moreau[d], Michael D. Cahalan[c,2], Pierre Vacher[b,3], and Patrick Legembre[a,2,3]

[a]Université Rennes-1, Institut de Recherche sur la Santé, l'Environnement et le Travail/Equipe Accueil Signalisation et Réponse aux agents infectieux et Chimiques 35043 Rennes, France; [b]Université Bordeaux Ségalen, Institut National de la Santé et de la Recherche Médicale U916, Institut Bergonié, 33076 Bordeaux, France; [c]Department of Physiology and Biophysics and Center for Immunology, University of California, Irvine, CA 92697; [d]Center National de la Recherche Scientifique UMR5164, 33076 Bordeaux, France; [e]Université Paul Sabatier, Institut National de la Santé et de la Recherche Médicale UMR1037, Centre de Recherches en Cancérologie de Toulouse, 31432 Toulouse, France; and [f]Institut National de la Santé et de la Recherche Médicale U1045, Centre de Recherche Cardio-Thoracique de Bordeaux, 33076 Bordeaux, France

Contributed by Michael D. Cahalan, October 13, 2011 (sent for review September 22, 2011)

The death receptor CD95 plays a pivotal role in immune surveillance and immune tolerance. Binding of CD95L to CD95 leads to recruitment of the adaptor protein Fas-associated death domain protein (FADD), which in turn aggregates caspase-8 and caspase-10. Efficient formation of the CD95/FADD/caspase complex, known as the death-inducing signaling complex (DISC), culminates in the induction of apoptosis. We show that cells exposed to CD95L undergo a reorganization of the plasma membrane in which the Ca^{2+} release-activated Ca^{2+} channel Orai1 and the endoplasmic reticulum-resident activator stromal interaction molecule 1 colocalize with CD95 into a micrometer-sized cluster in which the channel elicits a polarized entry of calcium. Orai1 knockdown and expression of a dominant negative construct (Orai1E106A) reveal that on CD95 engagement, the Orai1-driven localized Ca^{2+} influx is fundamental to recruiting the Ca^{2+}-dependent protein kinase C (PKC) β2 to the DISC. PKCβ2 in turn transiently holds the complex in an inactive status, preventing caspase activation and transmission of the apoptotic signal. This study identifies a biological role of Ca^{2+} and the Orai1 channel that drives a transient negative feedback loop, introducing a lag phase in the early steps of the CD95 signal. We suggest that these localized events provide a time of decision to prevent accidental cell death.

Fas | lymphocytes

The ubiquitously expressed death receptor CD95 (Fas/APO1) belongs to the TNF receptor family. CD95 and its cognate ligand CD95L are instrumental in immune surveillance and tolerance (1) and in the elimination of tumor cells exposed to radiotherapeutic and chemotherapeutic treatments (2). From a molecular standpoint, binding of CD95L to CD95 produces receptor clustering and formation of a polarized plasma membrane structure known as CD95-Cap (3). This membrane platform is crucial to promoting the recruitment of the adaptor protein Fas-associated death domain protein (FADD), which in turn aggregates caspase-8 and caspase-10. The CD95/FADD/caspase-8 complex is known as the death-inducing signaling complex (DISC) (4). The close proximity of these initiator caspases elicits their autoactivation and induction of the apoptotic signal.

Calcium ions (Ca^{2+}) participate in cell signaling as a second messenger that relies on intensity (cytosolic concentration), temporal parameters (i.e., duration and frequency), and spatial localization to trigger various cellular responses. In nonexcitable cells, Ca^{2+} responses occur mainly through a biphasic signal caused by activation of inositol 1,4,5-triphosphate (IP_3) receptors and the release of Ca^{2+} from the endoplasmic reticulum (ER), followed by a sustained Ca^{2+} entry across the plasma membrane (5). This store-operated Ca^{2+} entry (SOCE), mediated by Ca^{2+} release-activated Ca^{2+} (CRAC) channels, plays pivotal roles in both replenishment of the ER store and lymphocyte activation, leading to proliferation and cytokine production (6). Immune cells express a functional network of ion channels that play key roles in T-cell activation. Recently, stromal interaction molecule 1 (STIM1) was identified as the ER-stored Ca^{2+} sensor that links ER depletion to activation of the plasma membrane CRAC channel formed by Orai1 subunits, allowing Ca^{2+} to selectively enter the cell (7). After contact of a T cell with an antigen-presenting dendritic cell, STIM1 and Orai1 colocalize with T-cell receptors in the immunologic synapse and contribute to a localized Ca^{2+} influx (8). The molecular and functional roles of STIM1 and Orai1 in T lymphocytes have been reviewed previously (5, 9).

In addition to mediating T-cell activation via the nuclear factor of activated T cells gene expression pathway, Ca^{2+} also may play a role in T-cell apoptosis via CD95 signaling. Although an early report implicated extracellular Ca^{2+} in the CD95 signal (10), more recent data have challenged this involvement (11). In the present study, we examined the role of Ca^{2+} influx through Orai1 channels in the CD95 death pathway and showed that CD95 stimulation induces rapid relocalization of STIM1 and Orai1 into the CD95-Cap that leads to a polarized Ca^{2+} entry and recruits protein kinase C (PKC) β2 into the DISC. PKCβ2 in turn delays DISC formation and provides negative feedback for the cells exposed to the CD95L before their commitment toward cell death.

Results

CD95 Elicits a Ca^{2+} Signal Preventing the First Steps in Induction of the Apoptotic Signal. The addition of CD95L evoked a Ca^{2+} response consisting of an immediate rise to a peak followed by a sustained plateau in activated peripheral blood lymphocytes (PBLs) and leukemic T-cell lines H9 and Jurkat (Fig. 1*A* and Fig. S1 *A* and *B*). In contrast, T cells devoid of phospholipidase C, γ1 (PLCγ1) failed to mount a Ca^{2+} signal in the presence of CD95L, and phospholipase complementation restored the Ca^{2+} response (Fig. S1*C*). In addition, pretreatment of T cells with 2-

Author contributions: N.K., L.B.-B., P.V., and P.L. designed research; N.K., L.B.-B., A.P., B.C.-D., A.-M.V., and T.D. performed research; B.S., T.L., J.R., and M.D.C. contributed new reagents/analytic tools; N.K., L.B.-B., P.V., and P.L. analyzed data; and L.B.-B., J.-F.M., M.D.C., P.V., and P.L. wrote the paper.

The authors declare no conflict of interest.

[1]N.K. and L.B.B. contributed equally to this work.

[2]To whom correspondence may be addressed. E-mail: mcahalan@uci.edu or patrick.legembre@inserm.fr.

[3]P.V. and P.L. contributed equally to this work.

This article contains supporting information online at www.pnas.org/lookup/suppl/doi:10.1073/pnas.1116946108/-/DCSupplemental.

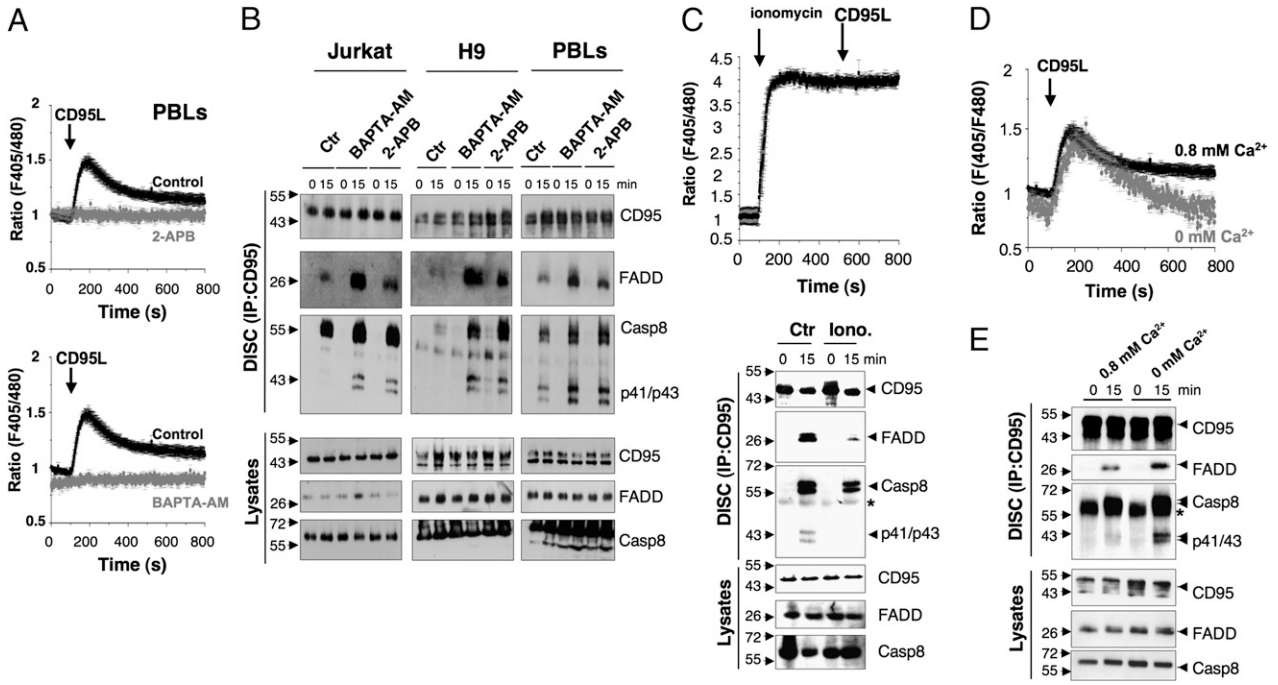

Fig. 1. CD95-mediated Ca^{2+} response prevents DISC formation. (*A*) Ca^{2+} response to CD95L (100 ng/mL) measured ratiometrically in suspensions of Indo-1–loaded activated PBLs. Cells were preincubated with BAPTA-AM (5 μM, *Upper*) or 2-APB (44 μm, *Lower*), or left untreated (control) before the addition of CD95L, indicated by the black arrow. The data represent mean ± SD of four independent experiments. (*B*) Jurkat, H9, and activated PBLs were pretreated as in *A* with BAPTA-AM, 2-APB, or DMSO (control), and then stimulated (15) for 15 min with the agonist anti-CD95 mAb APO1-3 (1 μg/mL) or left untreated (0). CD95 was immunoprecipitated, the immune complex was resolved by SDS/PAGE, and the indicated immunoblotting was performed. Total lysates were loaded as a control. p41/43 corresponds to the first step of caspase-8 cleavage. (*C*) Ca^{2+} signal and DISC formation in ionomycin-treated T cells. (*Upper*) Indo-1 ratiometric fluorescence in Jurkat T-cell suspensions exposed to ionomycin (1 μM) before stimulation with CD95L (100 ng/mL) at the indicated times. Data are mean ± SD of four independent experiments. (*Lower*) CD95 immunoprecipitation in Jurkat cells treated as in *C*, *Upper*. Data are representative of three independent experiments. (*D*) $[Ca^{2+}]_i$ in cell populations recorded with Indo-1 in activated PBLs stimulated with CD95L (100 ng/mL) in control medium (0.8 mM Ca^{2+}; black trace) or in medium containing BAPTA to chelate free Ca^{2+} (0.8 mM Ca^{2+} supplemented with 2 mM BAPTA; gray trace). Data represent mean ± SD of three independent experiments. The area under the curve corresponds to 321 ± 40 in regular medium 148 ± 37 in Ca^{2+}-free medium ($P < 0.001$). (*E*) DISC formation in activated PBLs preincubated for 30 min in medium containing 0.8 mM Ca^{2+} or medium supplemented with 2 mM BAPTA, then stimulated with APO1-3 (1 μg/mL). The star corresponds to the heavy chain of the APO1-3 IgG3.

aminoethoxydiphenyl borate (2-APB) (Fig. 1*A* and Fig. S1 *A* and *B*) and xestospongin C (Fig. S1*D*) totally abrogated the Ca^{2+} response. Together, these data suggest that generation of IP_3 by PLCγ1, ER Ca^{2+} release via the IP_3 receptor, and activation of CRAC channels underlie the CD95-triggered Ca^{2+} signal.

We next tested whether this rapid and transient increase in Ca^{2+} modulates the initial events of the CD95-mediated apoptotic signal. Inhibition of the CD95-mediated Ca^{2+} response by 2-APB, xestospongin C, or the intracellular Ca^{2+} chelator BAPTA-AM [1,2-bis-(*o*-aminophenoxy)ethane-*N*,*N*,*N*′,*N*′-tetraacetic acid tetra-(acetoxymethyl) ester] (Fig. 1*A* and Fig. S1 *A*–*D*) enhanced the binding of FADD to CD95 and subsequent DISC formation in activated PBLs and leukemic T-cell lines (Fig. 1*B* and Fig. S1*E*). Densitometric analyses of DISCs confirmed the inhibiting effect of Ca^{2+} on the initial steps of the CD95 signal (Fig. S1*F*). In addition, inhibition of the CD95-mediated Ca^{2+} response accelerated the process of caspase-8 cleavage, an early feature of the death receptor-mediated apoptotic signal (Fig. S2). To further confirm that the CD95L-triggered Ca^{2+} response interfered with DISC formation, we artificially increased the $[Ca^{2+}]_i$ in the Jurkat T-cell line using a noncytotoxic dose of the Ca^{2+} ionophore ionomycin and analyzed DISC formation after CD95L exposure. As anticipated, the increase in ionomycin-mediated $[Ca^{2+}]_i$ inhibited DISC formation (Fig. 1*C* and Fig. S3*A*). Collectively, these findings demonstrate that the CD95-mediated Ca^{2+} response blocks the initial steps of the CD95-mediated apoptotic signal.

To further address the contribution of Ca^{2+} influx to the CD95-mediated Ca^{2+} signal and its influence on the DISC formation, we compared the signal in cells bathed in Ca^{2+}-free medium. The area under the curve, taken as an indicator of the amplitude and duration of the CD95-mediated Ca^{2+} response, was reduced by 54% in activated PBLs bathed in a Ca^{2+}-free medium compared with control medium (Fig. 1*D*). Similar results were obtained with the leukemic T-cell lines H9 and Jurkat (Fig. S3 *B* and *C*), indicating that Ca^{2+} entry amplifies the CD95-mediated Ca^{2+} response in T lymphocytes. In addition, the absence of external Ca^{2+} significantly promoted DISC formation (Fig. 1*E* and Fig. S3*D*) and consequently enhanced the CD95-mediated apoptotic signal in Jurkat T cells (Fig. S3*E*). These findings demonstrate that Ca^{2+} entry is instrumental in preventing the recruitment of FADD and subsequent transmission of the apoptotic signal.

CD95-Mediated Ca^{2+} Influx by CRAC Channel Orai1. We next asked whether CRAC channels participate in the Ca^{2+} signal observed in cells exposed to CD95L. Treatment of the leukemic T-cell line H9 with the CRAC channel blocker BTP2 (12) abolished the sustained Ca^{2+} response (Fig. S3*F*) and enhanced DISC formation (Fig. S3*G*), but did not affect the initial Ca^{2+} mobilization that relied on proximal signaling and activation of the IP_3 receptor. Furthermore, in single-cell imaging experiments, adding back Ca^{2+} to cells bathed in a Ca^{2+}-free medium and prestimulated with CD95L resulted in a Ca^{2+} influx that was initially localized in the CD95-Cap in both activated PBLs (Fig. 2*A*) and Jurkat cells (Fig. S4*A*). In contrast, cells not exposed to CD95L exhibited a homogeneous and smaller increase in $[Ca^{2+}]_i$ (Fig. 2*A* and Fig. S4*A*). This localized Ca^{2+} entry suggests that CD95 engagement caused

PHYSIOLOGY

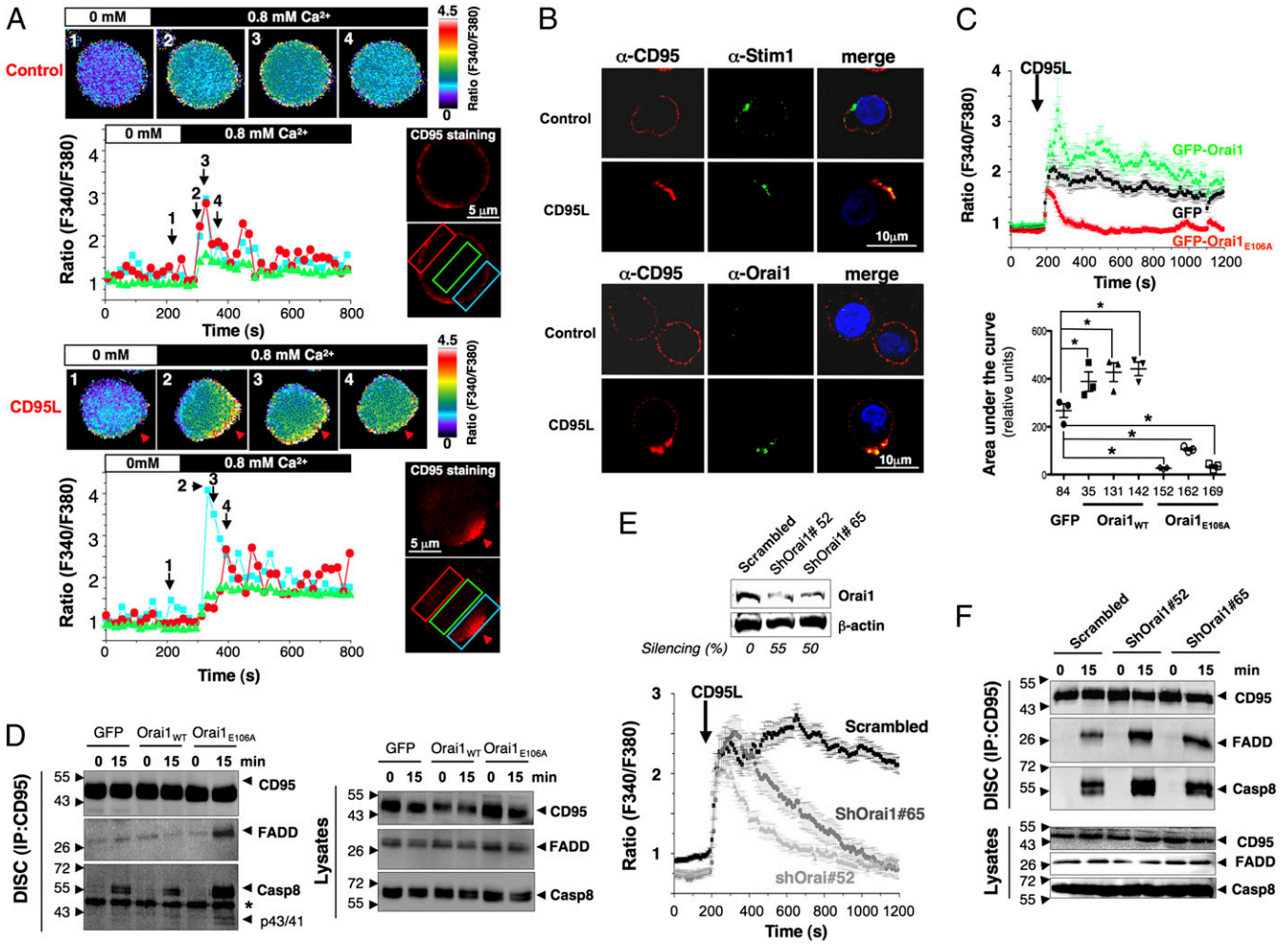

Fig. 2. STIM1/Orai1 distribution into the CD95-Cap triggers localized Ca^{2+} entry, impeding DISC formation. (*A*) Ca^{2+} influx colocalizes with CD95 at the DISC. In activated PBLs, CD95 was stained and untreated (*Upper*) or treated (*Lower*) with 100 ng/mL CD95L at 37 °C. CD95 labeling was analyzed using a conventional videomicroscopy setup (CD95 staining), and images of the fura-2PE3-AM fluorescence (F340nm/F380nm) were obtained every 5 s and translated into false colors according to the color scale shown on the right of the recorded cells. Cells were bathed in a Ca^{2+}-free extracellular medium (white bar), and 0.8 mM Ca^{2+}-containing medium was perfused in the bath (black bar) to visualize Ca^{2+} influx in CD95L-stimulated and unstimulated cells. For each condition, intracellular Ca^{2+} concentration was recorded at different time points. Black arrowheads and numbers in the histogram correspond to the above-annotated images. Red arrows indicate CD95-Cap. In the histograms, colored curves indicate the ratios (F340nm/F380nm) recorded in different areas of the activated PBLs depicted by colored rectangles. (*B*) Immunostaining showing colocalization of STIM1 and Orai1 with CD95. Activated PBLs were incubated in the presence or absence of CD95L (100 ng/mL) for 15 min. Cells were fixed and stained for CD95, STIM1, or Orai1. Nuclei are depicted in blue. Images were acquired with a confocal microscope using an Apoplan 63× objective. (*C*) Inhibition of Ca^{2+} entry by GFP-Orai1E106A. (*Upper*) $[Ca^{2+}]_i$ was assessed in Jurkat clonal cell lines expressing GFP alone (clone 84), GFP-Orai1 (clone 142), or GFP-Orai1E106A (clone 152) stimulated with 100 ng/mL of CD95L. The black arrow indicates addition of CD95L. Shown are the mean ± SD of more than 50 individual responses in Jurkat cells expressing GFP (black trace), GFP-Orai1E106A (red trace), or GFP-Orai1 (green trace). (*Lower*) Statistical analysis of the area under the curve for all isolated Jurkat clones in three independent experiments. $*P \leq 0.05$. (*D*) Immunoblot of DISC components in Jurkat T cells expressing GFP alone, GFP-Orai1, or GFP-Orai1E106A. Cells were incubated for 15 min with 1 μg/mL of APO1-3, and DISC components (*Left*) and total lysates (*Right*) were analyzed. These immunoblots are representative of three independent experiments. (*E*) ShRNA knockdown of Orai1 inhibits Ca^{2+} influx. (*Upper*) Jurkat cells infected with scrambled or two different Orai1-targeting shRNA lentiviruses were lysed, and the expression level of Orai1 was evaluated by immunoblot analysis. β-actin was used as a loading control. (*Lower*) $[Ca^{2+}]_i$ was determined as detailed in *A*. The mean ± SD of more than 30 individual responses to 100 ng/mL CD95L is shown. (*F*) Immunoblot of DISC components in cells described in *E*, stimulated for the indicated times with 1 μg/mL of APO1-3, and lysed to determine DISC formation. The data are representative of three independent experiments.

partitioning of this Ca^{2+} channel into the CD95-Cap. We then tested whether STIM1 and Orai1, constituting the CRAC channel in lymphocytes, participate in the localized Ca^{2+} entry observed in cells exposed to CD95L. Consistent with this hypothesis, confocal microscopy revealed that CD95 engagement triggered the migration of STIM1 and Orai1 into the CD95-Cap in primary T lymphocytes (Fig. 2*B*) and Jurkat T cells (Fig. S4*B*). To examine whether Orai1 is instrumental to the CD95-mediated Ca^{2+} influx, we generated Jurkat and CEM leukemic T cells stably expressing a dominant negative mutant of Orai1 (Orai1E106A). Orai1E106A expression was sufficient to inhibit the Ca^{2+} response in the presence of CD95L, compared with cells expressing GFP alone (Fig. 2*C* and Fig. S5 *A* and *B*). Conversely, overexpression of WT Orai1 caused an increased Ca^{2+} response on addition of CD95L (Fig. 2*C* and Fig. S5*B*). Similar results were found using the CEM T-cell line, ruling out any cell-specific effect (Fig. S5*C*).

DISC formation has been reported to occur inside the CD95-Cap (13), where we observed the greatest amount of Ca^{2+} in cells exposed to CD95L (Fig. 2*A* and Fig. S4*A*). Thus, we next explored whether Orai1 contributed to modulation of DISC formation. Although Orai1 overexpression significantly reduced DISC formation, ectopic expression of Orai1E106A dramatically enhanced

the recruitment of FADD and caspase-8 in the DISC (Fig. 2*D* and Fig. S5*D*). To confirm this latter result, Orai1 was silenced in the Jurkat T-cell line using a lentivirus-delivered Orai1-targeting shRNA. Although Orai1 knockdown did not interfere with initial Ca^{2+} mobilization, it did prevent the Ca^{2+} entry responsible for the sustained Ca^{2+} response (Fig. 2*E*). Confirming the data obtained with the dominant-negative mutant OraiE106A, DISC formation was improved in shRNAOrai1-expressing cells compared with the scrambled shRNA-transduced control cells (Fig. 2*F* and Fig. S5*E*). Taken together, these results demonstrate that CD95 stimulation triggers localized Ca^{2+} influx through the redistribution of STIM1/Orai1 into the CD95-Cap, and that this influx inhibits the initial steps of the CD95 signaling pathway.

Localized Orai1-Driven Ca^{2+} Entry Recruits PKCβ2 to the DISC. Inhibition of the DISC by the Ca^{2+} second messenger raised the question of what Ca^{2+}-dependent molecular target was contributing to the prevention of DISC formation. Previous studies have indicated that PKC activity alters the initial steps of the CD95 signal (14, 15); therefore, we tested whether the Orai1-mediated Ca^{2+} influx inhibited DISC formation by recruiting a Ca^{2+}-dependent PKC. Preincubation of activated T cells and Jurkat cells with enzastaurin, a PKCβ inhibitor (16), enhanced the CD95-mediated apoptotic signal (Fig. S6*A*), suggesting that this might be the isoform that prevents DISC formation. PKCβ1 and β2 are two Ca^{2+}-dependent alternatively spliced isoforms that differ only in their last 50 amino acid residues (17). Strikingly, exposure of activated PBLs or leukemic T cells to CD95L promptly elicited the relocalization of PKCβ2 from the cytoplasm to the CD95-Cap, whereas the distribution of PKCβ1 remained cytosolic (Fig. 3*A*). Moreover, PKCβ2 was found to coimmunoprecipitate within the DISC, whereas PKCβ1 was not detected in the complex (Fig. 3*B*).

We next explored the contribution of the entry of Orai1-driven Ca^{2+} to the redistribution of PKCβ2 to the CD95-Cap and DISC. Although PKCβ2 was localized within the CD95-Cap in GFP-Orai1–expressing T cells exposed to CD95L, inhibition of Ca^{2+} influx in Orai1E106A-expressing cells abrogated its transport to the plasma membrane (Fig. 3*C*). In agreement with this latter

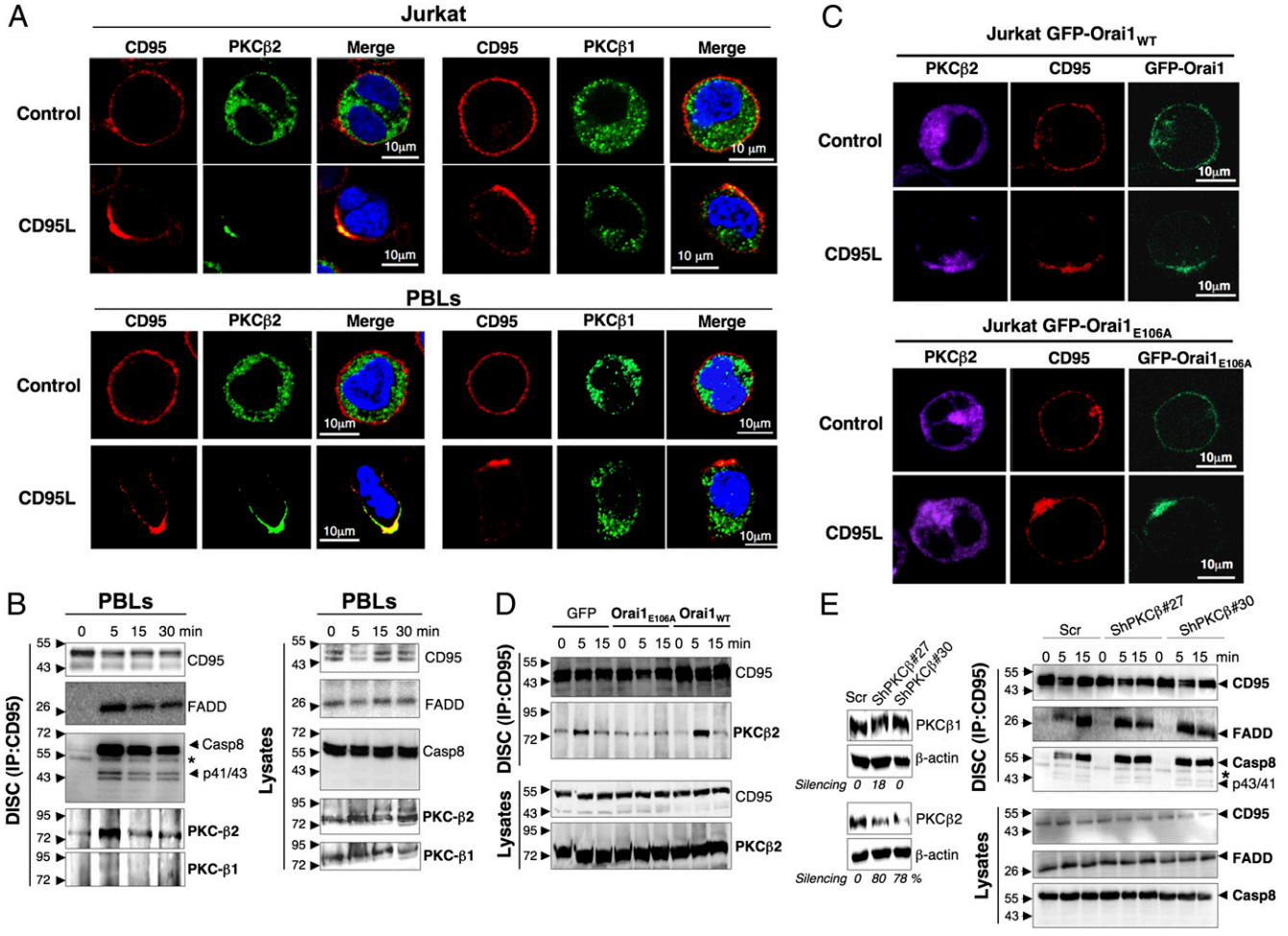

Fig. 3. Localized CD95-mediated Ca^{2+} entry redistributes PKCβ2 to the CD95-Cap. (*A*) Immunostaining of CD95, PKCβ1 (*Right*), or PKCβ2 (*Left*) in Jurkat T cells and activated PBLs that were untreated (control) or treated with 100 ng/mL CD95L for 15 min, fixed, and stained. Nuclei were stained using Hoechst 33248 (blue). Images were acquired with a confocal microscope with an Apoplan 63× objective. (*B*) Immunoblots of DISC components in activated PBLs incubated for the indicated times with 1 μg/mL of APO1-3 (*Left*). Total lysates were added as a control (*Right*). (*C*) Localization of CD95 and PKCβ2 in GFP-Orai1– and GFP-Orai1E106A–expressing Jurkat cells treated (CD95L) or untreated (control) for 15 min with 100 ng/mL of CD95L. Cells were fixed, permeabilized, and stained for CD95 and PKCβ2. Images were acquired as above. (*D*) Distribution of PKCβ2 in the DISC formed in GFP, GFP-Orai1E106A, and GFP-Orai1 Jurkat cells incubated for the indicated times with 1 μg/mL of APO1-3. (*E*) Immunoblot showing DISC components in cells after knockdown of PKC-β2. (*Left*) H9 T cells infected with lentivirus encoding scrambled ShRNA or two different PKC-β2–targeting ShRNAs were lysed, and the expression levels of PKCβ2 and β1 were assessed by immunoblot analysis. β-actin was added as a loading control. (*Right*) The aforementioned H9 T cells were incubated for the indicated times with 1 μg/mL of APO1-3, after which CD95 was immunoprecipitated and the DISC analyzed. Data are representative of three independent experiments.

observation, PKCβ2 was found in the DISC of parental and Orai1-overexpressing Jurkat cells, whereas it was barely detectable in the DISC of OraiE106A-expressing Jurkat cells (Fig. 3*D* and Fig. S6*B*). Collectively, these findings demonstrate that localized Orai1-driven Ca^{2+} entry promotes recruitment of PKCβ2 to the DISC.

Finally, to examine whether PKCβ2 alters the recruitment of FADD into the DISC, we knocked down expression of PKCβ2 using shRNA-encoding lentivirus and analyzed DISC formation. As expected, DISC formation was significantly accelerated in cells in which PKCβ2 expression was down-regulated (Fig. 3*E* and Fig. S6*C*), with a subsequent increase in sensitivity to the CD95-mediated apoptotic signal (Fig. S6*D*).

Ca^{2+} Entry Transiently Freezes Transmission of the CD95-Mediated Apoptotic Signal. Based on the transient Ca^{2+} response (Fig. 1*A*) and PKCβ2 recruitment in the DISC (Fig. 3*B*), we postulated that the CD95-mediated Ca^{2+} response could hold the DISC in an off position, allowing the apoptotic signal to be reversed, thereby providing a "time of decision" for the cells exposed to CD95L. To address this possibility, we incubated leukemic T-cell lines and PBLs with sufficient CD95L to kill 100% of the cells, and at different time points after the addition of CD95L, added saturating concentrations of the antagonist anti-CD95 antibody ZB4 to disrupt the CD95–CD95L interaction (Fig. S7*A*). For each condition, cell death was quantified after 6 h. Depending on the cells tested, the apoptotic signal could be reverted in 50% or more of the cells when the blocking anti-CD95 mAb was added at 1–50 min after initiation of the CD95–CD95L interaction (Fig. S7*B*). Given that DISC formation occurs between 1 and 50 min in the tested cells, we analyzed whether the duration of the time of decision varied as a function of Ca^{2+} entry using Orai1- and Orai1E106A-expressing T cells. Whereas blocking mAb enabled the rescue of half of the Jurkat-Orai1 cells for a delayed period (~70 min) compared with the parental counterpart (~32 min), the reversible state was significantly shortened in the OraiE106A-expressing Jurkat cells (~20 min) (Fig. 4*A*). Overall, these findings demonstrate that in cells exposed to CD95L, Orai1-driven Ca^{2+} entry delays delivery of the apoptotic signal.

Discussion

This study has addressed the role of Orai1 channels and subsequent Ca^{2+} entry in the proximal CD95-driven sequence of events leading to apoptosis in T lymphocytes. We have shown that stimulation of CD95 by the cytotoxic cytokine CD95L evokes a biphasic Ca^{2+} signal lasting several minutes, composed of an early peak followed by a sustained phase. The transient peak occurs through the activation of PLCγ1, which in turn leads to the activation of IP_3 receptors and mobilization of the ER-stored Ca^{2+}. Our study demonstrates the pivotal role of the Orai1 channel in mediation of SOCE that gives rise to the sustained Ca^{2+} response in cells exposed to CD95L. In addition, our results show that the CD95-mediated Ca^{2+} influx is localized primarily within the CD95-Cap, where the divalent ion orchestrates the inhibition of the forming DISC.

Localized Ca^{2+} signaling through Orai1 was previously demonstrated in the zone of contact between T cells and antigen-presenting dendritic cells in the immunologic synapse (8). Similarly, our study demonstrates that local Ca^{2+} signals occur during the formation of CD95-Cap, a polarized and micrometer-sized platform that brings together proteins of the forming DISC complex and the CRAC channel STIM1/Orai1. Ca^{2+} entry through Orai1 channels would result in steep concentration gradients produced rapidly and focally to much higher levels than the bulk cytoplasmic Ca^{2+} (18, 19). Thus, the localization of appropriate targets close to the Ca^{2+} channels would result in rapid and selective activation or inhibition of downstream Ca^{2+}-dependent events (20). We show that CD95 engagement drives the formation of a CD95-Cap overlapping with STIM1 and Orai1 mirror clusters induced by ER store depletion. This functional coupling between the DISC and STIM1/Orai1 suggests close proximity, although direct protein–protein interactions were not detected. The resulting Ca^{2+} rise freezes the DISC by impeding the sequence of events that normally would lead to the formation of a functional complex. Consequently, the CD95-mediated Ca^{2+} signal behaves as a negative feedback loop whose likely function is to bring together the forming DISC and Ca^{2+}-modulated factors.

Although members of the PKC family have been reported to prevent induction of the CD95 signal (14, 21), the possibility of

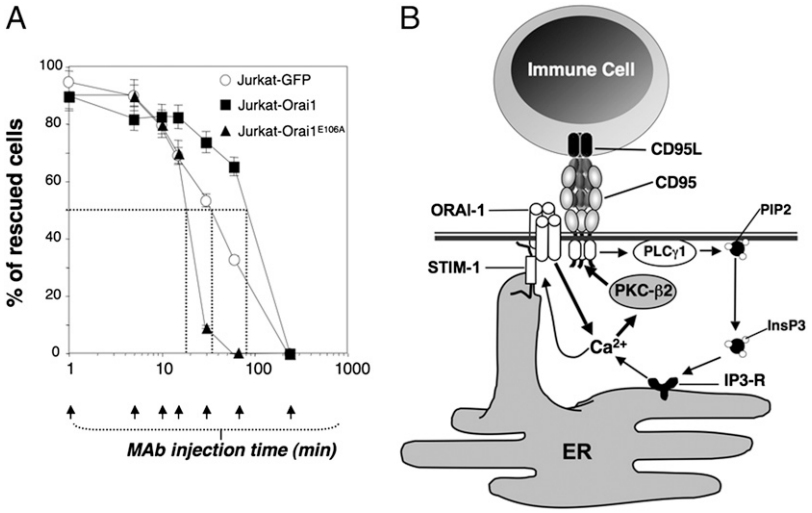

Fig. 4. Orai1-driven Ca^{2+} entry delays the irreversible induction of the CD95-mediated apoptotic signal. (*A*) Kinetics of death induction measured by mitochondrial potential, delayed by overexpression of Orai1 and accelerated by expression of Orai1E106A. The indicated cells were incubated for 6 h with 10 ng/mL of CD95L, a concentration that triggers 100% cell death in Jurkat-GFP cells. Blocking anti-CD95 mAb ZB4 or isotype control mAb (2.5 μg/mL) was added at the indicated times. Cell death was assessed after 6 h by measuring the decrease in $\Delta\Psi m$. The percentage of "rescued cells" was estimated as follows: [100 – (dead cells with blocking anti-CD95 mAb/dead cells with isotype control mAb) × 100]. (*B*) Schematic summary of the CD95-mediated Ca^{2+} response. CD95 engagement elicits the PLCγ1 activation, which in turn mobilizes the ER-stored Ca^{2+} through IP_3 receptor activation, leading to STIM1/Orai1-driven entry of Ca^{2+}. The localized Ca^{2+} entry redistributes PKCβ2 to the CD95-Cap, where the kinase activity hinders DISC formation.

Ca^{2+}-dependent isoforms altering the CD95-mediated apoptotic signal was ruled out based on the paradigm that an increase in $[Ca^{2+}]_i$ behaves as a general and potent catalyst of cell death (22). In light of our current findings, this paradigm must be revisited. We propose that the Orai1-driven Ca^{2+} entry occurring beneath the CD95-Cap recruits PKCβ2 to the plasma membrane, where the kinase promptly but transiently associates with the newly constituted DISC and provides a time of decision for bystander cells to avoid their accidental elimination by the CD95L-loaded immune cells. This sequence of events is summarized in Fig. 4*B*.

We recently showed that in contrast to the proapoptotic membrane-bound CD95L, the metalloprotease-processed CD95L fragment fails to trigger an apoptotic signal in activated T lymphocytes and tumor cells, but rather orchestrates a Ca^{2+}-dependent migratory signal in these cells (23). In light of these recent observations, it may be argued that regardless of the type of CD95L (i.e., soluble or membrane-bound) to which cells are exposed, the CD95-mediated Ca^{2+} response controls the initial steps in the receptor signaling pathway to promote the transmission of nonapoptotic signals. In other words, Ca^{2+} switches CD95 from an apoptotic receptor to a nonapoptotic receptor, and thus may account for the recently reported pro-oncogenic role of CD95 in lung, liver and ovarian cancers (24, 25).

Materials and Methods

Cell Lines and PBLs. Human CEM, H9, and Jurkat T-leukemic cell lines were maintained in RPMI supplemented with 8% vol/vol heat-inactivated FCS and 2 mM L-glutamine at 37 °C in a 5% CO_2 incubator. Peripheral blood mononuclear cells from healthy donors were isolated by Ficoll centrifugation. Monocytes were depleted by a 2-h adherence step, and the naive PBLs were stimulated as described previously (23). Selection of clonal cell lines overexpressing GFP-tagged Orai1 and GFP-Orai1E106A and shRNA silencing experiments are described in *SI Materials and Methods*.

Ca^{2+} Monitoring. In cell populations, $[Ca^{2+}]_i$ was measured ratiometrically in Indo-1–loaded cells using a Hitachi F2500 spectrophotometer, as described previously (26). Cells bathed in HBSS were placed in a quartz cuvettete under continuous stirring. The Indo-1 fluorescence response to $[Ca^{2+}]_i$ was recorded as the F405nm/F480nm fluorescence ratio. Each experimental condition was repeated independently at least three times; values are reported as mean ± SD. Single-cell $[Ca^{2+}]_i$ imaging was performed ratiometrically as described previously (23). Cells were loaded with 5 μM fura 2-PE3-AM for 30 min at room temperature in HBSS solution; CD95 was simultaneously stained using DX2, a nonagonistic anti-CD95 mAb (1 μg/mL). Cells were then washed and incubated for 30 min with an Alexa Fluor 555-conjugated goat anti-mouse mAb. CD95-stained cells were untreated or treated with 100 ng/mL of CD95L at 37 °C. Fura 2-PE3-AM exhibits limited compartmentalization in intracellular stores and is leakage-resistant (27). For certain cells, regions of interest were drawn on the recorded cells to restrict data collection to specific regions. Imaging was controlled by Universal Imaging software, including MetaFluor and MetaMorph. All images were background-subtracted. Data processing was performed using OriginPro 7.5 software (Origin Lab). For each condition, cells with spontaneous Ca^{2+} activity were identified by imaging and eliminated from the analysis. Each depicted cell is representative of a minimum of five independent experiments.

Western Blot Analysis, DISC Analysis, and Subcellular Localization. Expression of Orai1, PKCβ1, and PKCβ2 in T-cell lines infected with shRNA-expressing lentivirus was assessed by Western blot analysis, as described in *SI Materials and Methods*. For DISC analysis, CD95 was immunoprecipitated as described in *SI Materials and Methods*, and the immune complex was assessed by Western blot analysis. Localization of CD95, Orai1, STIM1, PKCβ1, and PKCβ2 was done using a Zeiss LSM 510 META confocal microscope, as described in *SI Materials and Methods*.

Cell Death Assays. Cell viability was assessed using the MTT assay (28) or measurement of mitochondrial potentials ($\Delta\Psi m$), as described previously (29) and detailed in *SI Materials and Methods*.

ACKNOWLEDGMENTS. We thank Dr. J. Le Seyec and Dr. P. Gripon for their technical support with lentivirus productions (L3 facilities, IFR140, Rennes). This work was supported by Agence Nationale de la Recherche (ANR JC07_183182), Institut National du Cancer (Projets Libres Recherche Biomédicale), Cancéropole Grand Ouest, Région Bretagne, Rennes Métropole, Université de Rennes-1, Ligue Contre le Cancer (Comités d'Ille-et-Vilaine/du Morbihan/des Côtes d'Armor/du Maine et Loire/des Landes), and the National Institutes of Health (Grant NS-14609, to M.D.C.). N.K. is supported by Region Bretagne (Allocation de Recherche Doctorale).

1. Strasser A, Jost PJ, Nagata S (2009) The many roles of FAS receptor signaling in the immune system. *Immunity* 30:180–192.
2. Debatin KM, Krammer PH (2004) Death receptors in chemotherapy and cancer. *Oncogene* 23:2950–2966.
3. Cremesti A, et al. (2001) Ceramide enables fas to cap and kill. *J Biol Chem* 276: 23954–23961.
4. Kischkel FC, et al. (1995) Cytotoxicity-dependent APO-1 (Fas/CD95)-associated proteins form a death-inducing signaling complex (DISC) with the receptor. *EMBO J* 14: 5579–5588.
5. Oh-hora M, Rao A (2008) Calcium signaling in lymphocytes. *Curr Opin Immunol* 20: 250–258.
6. Qian D, Weiss A (1997) T cell antigen receptor signal transduction. *Curr Opin Cell Biol* 9:205–212.
7. Cahalan MD (2009) STIMulating store-operated Ca(2+) entry. *Nat Cell Biol* 11:669–677.
8. Lioudyno MI, et al. (2008) Orai1 and STIM1 move to the immunological synapse and are up-regulated during T cell activation. *Proc Natl Acad Sci USA* 105:2011–2016.
9. Cahalan MD, Chandy KG (2009) The functional network of ion channels in T lymphocytes. *Immunol Rev* 231:59–87.
10. Hampton MB, Vanags DM, Pörn-Ares MI, Orrenius S (1996) Involvement of extracellular calcium in phosphatidylserine exposure during apoptosis. *FEBS Lett* 399:277–282.
11. Wozniak AL, et al. (2006) Requirement of biphasic calcium release from the endoplasmic reticulum for Fas-mediated apoptosis. *J Cell Biol* 175:709–714.
12. Zitt C, et al. (2004) Potent inhibition of Ca^{2+} release-activated Ca^{2+} channels and T-lymphocyte activation by the pyrazole derivative BTP2. *J Biol Chem* 279:12427–12437.
13. Algeciras-Schimnich A, et al. (2002) Molecular ordering of the initial signaling events of CD95. *Mol Cell Biol* 22:207–220.
14. Drew L, Kumar R, Bandyopadhyay D, Gupta S (1998) Inhibition of the protein kinase C pathway promotes anti-CD95–induced apoptosis in Jurkat T cells. *Int Immunol* 10: 877–889.
15. Ruiz-Ruiz C, Robledo G, Font J, Izquierdo M, López-Rivas A (1999) Protein kinase C inhibits CD95 (Fas/APO-1)-mediated apoptosis by at least two different mechanisms in Jurkat T cells. *J Immunol* 163:4737–4746.
16. Green LJ, et al. (2006) Development and validation of a drug activity biomarker that shows target inhibition in cancer patients receiving enzastaurin, a novel protein kinase C-β inhibitor. *Clin Cancer Res* 12:3408–3415.
17. Kubo K, Ohno S, Suzuki K (1987) Primary structures of human protein kinase C-βI and -βII differ only in their C-terminal sequences. *FEBS Lett* 223:138–142.
18. Luik RM, Wu MM, Buchanan J, Lewis RS (2006) The elementary unit of store-operated Ca^{2+} entry: Local activation of CRAC channels by STIM1 at ER–plasma membrane junctions. *J Cell Biol* 174:815–825.
19. Wu MM, Buchanan J, Luik RM, Lewis RS (2006) Ca^{2+} store depletion causes STIM1 to accumulate in ER regions closely associated with the plasma membrane. *J Cell Biol* 174:803–813.
20. Berridge MJ, Bootman MD, Roderick HL (2003) Calcium signalling: Dynamics, homeostasis and remodelling. *Nat Rev Mol Cell Biol* 4:517–529.
21. Ruiz-Ruiz MC, Izquierdo M, de Murcia G, López-Rivas A (1997) Activation of protein kinase C attenuates early signals in Fas-mediated apoptosis. *Eur J Immunol* 27: 1442–1450.
22. Nicotera P, Orrenius S (1998) The role of calcium in apoptosis. *Cell Calcium* 23: 173–180.
23. Tauzin S, et al. (2011) The naturally processed CD95L elicits a c-yes/calcium/PI3K–driven cell migration pathway. *PLoS Biol* 9:e1001090.
24. Bivona TG, et al. (2011) FAS and NF-κB signalling modulate dependence of lung cancers on mutant EGFR. *Nature* 471:523–526.
25. Chen L, et al. (2010) CD95 promotes tumour growth. *Nature* 465:492–496.
26. Sorin B, et al. (1998) Distinct cytoplasmic regions of the prolactin receptor are required for prolactin-induced calcium entry. *J Biol Chem* 273:28461–28469.
27. Vorndran C, Minta A, Poenie M (1995) New fluorescent calcium indicators designed for cytosolic retention or measuring calcium near membranes. *Biophys J* 69: 2112–2124.
28. Legembre P, Moreau P, Daburon S, Moreau JF, Taupin JL (2002) Potentiation of Fas-mediated apoptosis by an engineered glycosylphosphatidylinositol-linked Fas. *Cell Death Differ* 9:329–339.
29. Chaigne-Delalande B, Mahfouf W, Daburon S, Moreau JF, Legembre P (2009) CD95 engagement mediates actin-independent and -dependent apoptotic signals. *Cell Death Differ* 16:1654–1664.